AIChE WILEY InterScience DISCOVER SOMETHING GREAT

PROCESS SYSTEMS ENGINEERING

Optimal Grade Transition in Industrial Polymerization Processes via NCO Tracking

J. V. Kadam and W. Marquardt
Lehrstuhl für Prozesstechnik, RWTH Aachen University, Turmstr. 46, D-52064 Aachen, Germany

B. Srinivasan and D. Bonvin
Laboratoire d'Automatique, École Polytechnique Fédérale de Lausanne, CH-1015 Lausanne, Switzerland

DOI 10.1002/aic.11085
Published online February 6, 2007 in Wiley InterScience (www.interscience.wiley.com).

In industrial polymerization processes, several grades of polymer are frequently produced in the same plant by changing the operating conditions. Transitions between the different grades are rather slow and result in the production of a considerable amount of off-specification polymer. Grade transition improvement is viewed here as a dynamic optimization problem, for which numerous approaches exist. Open-loop implementation of the input profiles obtained from numerical optimization of a nominal process model is often insufficient, due to the presence of uncertainty in the form of model mismatch and process disturbances. A novel measurement-based approach that consists of tracking the necessary conditions of optimality (NCO tracking) using a solution model and measurements is considered. The solution model consists of state-event-triggered controllers sequenced according to the structure of the nominal optimal solution computed offline. The solution model is generated by expressing the input profiles in terms of arcs and switching times, which are then related to the various parts of the NCO, that is, to the active constraints and sensitivities. These arcs and switching times are then adapted online using appropriate measurements. The application of NCO tracking to an industrial polymerization process for implementing optimal grade transitions is investigated in simulation. The grade transition problem is fairly complex due to a large-scale process model, many degrees of freedom, as well as path and endpoint constraints. A solution model is generated from the nominal optimal solution, and a control superstructure is considered to handle the possible activation of nominally-inactive constraints. Simple PI-type controllers are used to implement the solution model. For different uncertainty scenarios, simulation of the NCO-tracking approach shows that considerable reduction in transition time is possible, while still guaranteeing feasible operation. © 2007 American Institute of Chemical Engineers *AIChE J,* 53: 627–639, 2007

Keywords: dynamic real-time optimization, necessary conditions of optimality, self-optimizing control, constraint tracking, grade change, polymerization

Introduction

The worldwide production of synthetic polymers exceeds 100 million tons per year with their many different grades and prices. While on the one hand the product specifications for high-value products become tighter and tighter, on the other hand many of the specialty polymers are becoming

Correspondence concerning this article should be addressed to W. Marquardt at marquardt@lpt.rwth-aachen.de

Present address of J.V. Kadam: ExxonMobil Chemical Company, Manufacturing and Engineering Services- Process Control, Canadastraat 20, 2070 Zwijndrecht, Belgium.

Present address of B. Srinivasan: Department of Chemical Engineering, Ecole Polytechnique Montreal, Montreal, Canada H3C 3A7.

commodities resulting in lower profit margins, thus, requiring an efficient and cost-effective production. Furthermore, the highly fluctuating demands of the global market call for very flexible process operation with frequent changes in polymer grade, production load and product quality. Thus, for the polymer industries, the competitive edge will essentially come from the technologies that excel in controlling the polymer properties in a consistent way, while concurrently and flexibly satisfying the market demand and improving the economical performance. Besides the economical aspects, the intrinsic characteristics of polymerization processes pose challenging problems of operation, control and optimization.

Three distinct types of operational problems in the polymer industry are usually encountered. The most common problem is the *quality control problem.* The main task consists of keeping the quality-relevant variables at their desired setpoints, despite disturbances, in order to stay within the bounds specified by the end-user properties. Disturbances can either be general stochastic process disturbances, for example, changing feed properties, or disturbances forced on the process by the operational policy, for example, changes of production load or product grades. The second problem, referred to as the *grade change problem,* actually corresponds to one of these disturbance scenarios. Most polymerization plants, even though being continuous plants, produce several grades of polymer per production line. These grade changes tend to become more and more frequent due to tighter requirements imposed by market demands and supply chain optimization. During the transition from one grade to another, the plant in most cases produces a certain amount of off-specification material. One major task for improving the economics of the process is to determine optimal operational trajectories that minimize the amount of off-specification polymer (in many cases equivalent to the minimization of the transition time). The third problem is the *load change problem*, which can also be considered as disturbance rejection for quality control.

A large number of publications dealing with control and optimization of polymerization processes can be found in the literature (see for example, Embirucu et al. (1996), Congalidis and Richards (1998) for a general review). The quality control problem is often considered and, in most cases, model predictive control (MPC) technology is proposed for ensuring the quality (for example, Ogunnaike (1994), Mutha et al. (1997), Prasad et al. (2002), Na and Rhee (2002), Young et al. (2002)). Despite the large number of recent articles dealing with various aspects of polymerization reactor control, most of these publications are from a relatively small number of active academic groups. Furthermore, given the highly competitive and proprietary nature of commercial polymerization manufacturing technologies, it is not surprising that contributions from industrial practitioners are rather limited (Congalidis and Richards, 1998). A small number of industrial applications have been published, mainly regarding polyolefine processes (for example, McAuley and MacGregor (1991), Böhm et al. (1992), Kiparissides et al. (1997), Dittmar and Martin (1997), Seki et al. (1994)).

Off-line dynamic optimization problems have been formulated and solved for polymer grade transitions (for example, McAuley and MacGregor (1992)). Even though offline optimization may be routinely performed, concepts for its integration into operation are largely non-existent in industry. Several reasons for this situation can be identified:

- For most industrial processes, the *initial state* at the beginning of a transition is unknown due to lack of measurements. The initial state needs to be inferred from measurements using state estimation techniques, which would significantly increase the complexity of the approach.
- The offline dynamic optimization is based on an uncertain process model due to *plant-model mismatch.* It is typically not clear whether the model is sufficiently accurate to apply a trajectory computed via offline optimization without additional feedback via a quality controller.
- If the numerical optimization problem cannot be solved on site during plant operation, a *combinatorial problem* results. In this case, trajectories have to be precomputed for all possible combinations of desired grades and initial conditions, and stored in a database from where they can be retrieved during plant operation to implement a desired grade transition.

Any on-line strategy for implementation of an optimal grade transition has to build on a sufficient number of reliable measurements. Although there has been significant improvement in sensor technologies for polymerization processes, the availability of reliable measurements, in particular of polymer quality, is still a major challenge. Yet, the available measurements have not been fully exploited for optimal operation of polymerization processes in daily production using real-time optimization. For this goal, two measurement-based approaches, shown in Figures 1 and 2, can be considered:

1. *Approach based on a process model.* Here, the measurements (y) are used to estimate on-line the current state ($\hat{x}$), and disturbances (d). The inputs (u) are updated by repeatedly solving an online optimization problem that utilizes a dynamic model of the process. This approach is referred to as *single level dynamic real-time optimization* (D-RTO) (Kadam et al., 2002). Its structure is identical to nonlinear model predictive control (NMPC) with output feedback (Diehl et al., 2002). However, it relies on an economical objective function rather than some set-point deviation metric. It is shown in Figure 1. For large-scale industrial applications, the D-RTO problem is computationally expensive to solve though significant progress has been made in recent years (for example, Bock et al. (2000), Biegler et al. (2002), Schlegel et al. (2005)), and will continue to be made in the future. Due to the considerable computational requirements,

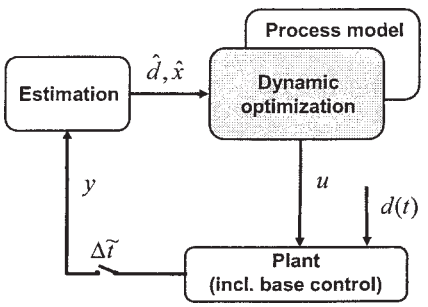

Figure 1. Single level D-RTO using a process model.

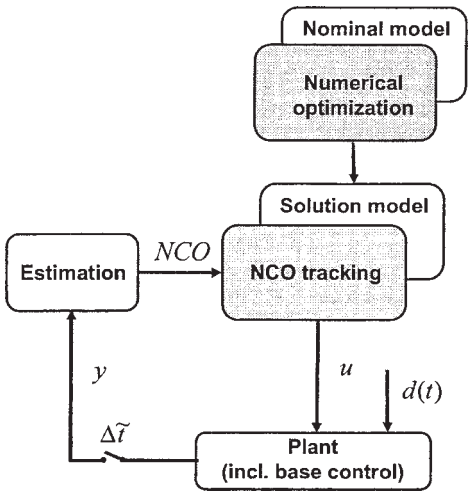

Figure 2. D-RTO via numerical optimization of a nominal model and NCO tracking.

large sampling intervals (Δt) are necessary for large-scale problems, which may not be acceptable due to model or process uncertainty. Furthermore, the failure of any on-line optimization could affect process safety and performance. Due to the complexity of D-RTO, its acceptance in industry is limited at this point in time. Though the situation will improve in the future due to advances in optimization technology, and the expected availability of commercial tools, alternative approaches that do not require online numerical optimization should be investigated.

2. *Approach based on a solution model*. This alternative, which is conceptually different from the previous approach, is shown in Figure 2. It employs measurements (y) to directly update the inputs (u) using a parameterized solution model that has been obtained from the offline numerical solution of the dynamic optimization problem using a nominal model (Srinivasan et al., 2003a). The approach is labelled *NCO tracking* as it attempts to meet the necessary conditions of optimality (NCO) for the dynamic optimization problem. The details of the approach are presented in the Optimal Grade Transition via NCO Tracking section.

The NCO-tracking approach is considered for application to a large industrial polymerization process involving grade transitions. The focus of this article is on demonstrating the applicability of NCO tracking for a class of perturbations.

This article is organized as follows. In the Preliminaries section, basic material regarding the general dynamic optimization problem and its solution is presented. The off-specification NCO-tracking approach is also introduced in this section. The industrial polymerization process is described in the Industrial Polymerization Process section, while the optimal grade change problem is formulated and solved for the nominal case in the Grade Transition via Numerical Optimization section. The proposed solution model and the NCO-tracking results for different uncertainty realizations are presented in the Optimal Grade Transition via NCO Tracking section. Finally, concluding remarks are proposed in the Conclusion.

Preliminaries

Problem formulation

We consider the following terminal-cost dynamic optimization problem

$$\min_{\boldsymbol{u}(t),t_f} \Phi(\boldsymbol{x}(t_f),t_f) \tag{P1}$$

$$\text{s.t.} \quad \dot{\boldsymbol{x}} = \boldsymbol{f}(\boldsymbol{x},\boldsymbol{u}), \quad \boldsymbol{x}(t_0) = \boldsymbol{x}_0, \tag{1}$$

$$\boldsymbol{0} \geq \boldsymbol{h}(\boldsymbol{x},\boldsymbol{u}), \tag{2}$$

$$\boldsymbol{0} \geq \boldsymbol{e}(\boldsymbol{x}(t_f)), \tag{3}$$

where $\boldsymbol{x}(t) \in \mathbb{R}^{n_x}$ denotes the vector of state variables with the initial conditions $\boldsymbol{x}_0$. The algebraic equations in the original differential-algebraic process model are assumed to be solved for the algebraic variables, which are then eliminated in the differential equations to result in Eq. 1. The time-dependent input variables $\boldsymbol{u}(t) \in \mathbb{R}^{n_u}$ and possibly the final time are the decision variables for optimization. Furthermore, there are path constraints $\boldsymbol{h}$ on the input and state variables in Eq. 2, and endpoint constraints $\boldsymbol{e}$ on the state variables in Eq. 3. Note that all functions involved in (P1) have to be sufficiently smooth.

There exist numerous solution techniques for dynamic optimization problems of the form (P1) (Binder et al. 2001). In this work, we use the sequential or single-shooting approach, a direct method that solves the problem by transcribing it into a nonlinear programming problem (NLP) through parameterization of the input variables $\boldsymbol{u}(t)$. For this purpose, we employ the algorithm with efficient adaptation techniques implemented in the software tool DyOS (Schlegel et al., 2005; Schlegel and Marquardt, 2006a; Schlegel and Marquardt, 2006b).

Necessary conditions of optimality

By using Pontryagin's minimum principle (Bryson and Ho, 1975), problem (P1) can be reformulated with the *Hamiltonian* function $H(t)$ as

$$\min_{u(t),t_f} H(t) = \boldsymbol{\lambda}^T \boldsymbol{f}(\boldsymbol{x},\boldsymbol{u}) + \boldsymbol{\mu}^T \boldsymbol{h}(\boldsymbol{x},\boldsymbol{u}) \tag{P2}$$

$$\text{s.t.} \quad \dot{\boldsymbol{x}} = \boldsymbol{f}(\boldsymbol{x},\boldsymbol{u}), \quad \boldsymbol{x}(t_0) = \boldsymbol{x}_0, \tag{4}$$

$$\dot{\lambda}^T = -\frac{\partial H}{\partial x}, \lambda^T(t_f) = \left(\frac{\partial \Phi}{\partial \boldsymbol{x}} + \boldsymbol{v}^T \frac{\partial e}{\partial \boldsymbol{x}}\right)\Bigg|_{t_f} \tag{5}$$

$$0 = \boldsymbol{\mu}^T \boldsymbol{h}(\boldsymbol{x},\boldsymbol{u}) \tag{6}$$

$$0 = \boldsymbol{v}^T \boldsymbol{e}(\boldsymbol{x}(t_f)) \tag{7}$$

Here, $\boldsymbol{\lambda}(t) \neq \boldsymbol{0}$ denotes the adjoint variables, $\boldsymbol{\mu}(t) \geq \boldsymbol{0}$ and $\boldsymbol{v} \geq \boldsymbol{0}$ the Lagrange multipliers for the path and endpoint constraints, respectively. The complementarity conditions, Eqs. 6–7 indicate that a Lagrange multiplier is positive if the corresponding constraint is active and zero otherwise.

An optimal solution of problem (P2) fulfills the necessary conditions of optimality

$$\frac{\partial H(t)}{\partial \boldsymbol{u}} = \boldsymbol{0} \tag{8}$$

Table 1. Separation of the NCO into Four Distinct Parts

	Path Objectives	Terminal Objectives
Constraints	$\mu^T h = 0$	$v^T e = 0$
Sensitivities	$\frac{\partial H}{\partial u} = 0$	$H(t_f) + \frac{\partial \Phi}{\partial t}\Big\|_{t_f} = 0$

If a free final time is allowed, the additional transversality condition

$$H(t_f) = -\frac{\partial \Phi}{\partial t}\bigg|_{t_f} \tag{9}$$

has to be satisfied as well. The necessary conditions can be rewritten in the partitioned form of Table 1 by separating (i) the conditions linked to the active constraints from those related to sensitivities (first and second rows in Table 1), and (ii) the conditions linked to path objectives from those related to terminal objectives (first and second columns in Table 1).

NCO tracking using a solution model

NCO tracking adjusts the manipulated variables by means of a decentralized control scheme in order to meet the necessary conditions of optimality (NCO) for the real plant. This way, nearly optimal operation can be implemented via feedback control without the need for solving a dynamic-optimization problem in real-time. The real challenge lies in the fact that four different objectives (Table 1) are involved in achieving optimality. These objectives are linked to active constraints (Eqs. 6 and 7) and sensitivities (Eqs. 8 and 9). Hence, it becomes important to appropriately parameterize the inputs using both time functions and time-invariant parameters, and assign them to the different objectives. The result is a solution model, that is, a decentralized self-optimizing control scheme, that relates the available decision variables (seen as manipulated inputs) to the NCO (seen as controlled outputs) given in Table 1.

The generation of a solution model includes two main steps (Srinivasan and Bonvin, 2004)

• *Input dissection.* The input dissection step starts with the numerical optimization of a nominal process model. The resulting optimal solution is typically discontinuous and consists of various arcs or intervals (Bryson and Ho, 1975; Srinivasan et al., 2003b). This information on the type of arcs is obtained from the numerical solution of the optimization problem (P1). Schlegel and Marquardt (2006b) have proposed a method that automatically detects the control switching structure.

An important feature is the use of an input parameterization that takes the active constraints into consideration. Some of the arcs are parameterized using a piecewise-polynomial approximation, while others (especially those characterized by active path constraints) are left as infinite-dimensional variables. Also, since the inputs are typically discontinuous, it is helpful to treat the switching times as explicit decision variables. Consequently, the decision variables $u(t)$ and t_f in problem (P2) can be parameterized as

$$\boldsymbol{u}(t) = \mathcal{U}(\eta(t), \tau) \tag{10}$$

where $\eta(t)$ are the time-varying control profiles that are left as infinite-dimensional variables, and τ the switching times.

• *Linking the decision variables to the NCO.* The next step is to provide a link between the decision variables and the NCO elements given in Table 1. The active path and terminal constraints fix some of the time functions $\eta(t)$ and switching times τ, respectively. The remaining degrees of freedom are used to meet the path and terminal sensitivities. Though the pairing of decision variables and NCO is not unique, it has been found recently that optimal pairing is not critical in many applications (Srinivasan and Bonvin, 2006). An important assumption here is that the set of active constraints is correctly determined and does not vary with uncertainty. Fortunately, this restrictive assumption can often be relaxed by considering a *superstructure of the solution model,* which takes into account possible changes in the nominally active constraints set, as will be illustrated in the Grade Transition via Numerical Optimization section.

Once a solution model has been postulated, it provides the basis for adapting the decision variables using appropriate controllers and measurements of the NCO parts. However, the solution model does not specify whether a controller is implemented online or in a run-to-run fashion. Online implementation requires reliable online measurements or estimation of the corresponding NCO parts. Often, measurements of the constrained variables are available online. When online measurements of certain NCO parts are not available (for example, sensitivities and terminal constraints), a model-based estimator can be used to predict them. Otherwise, a run-to-run implementation that uses measurements at the end of the run becomes necessary.

At this point, it is important to mention that there exists no complete and systematic procedure for deriving a solution model, Physical insight is necessary as it helps characterize the optimal nominal solution, choose an appropriate pairing of manipulated and controlled variables, and decide on the feedback implementation type (online or run-to-run). Initial experiences have been made with various processes that include semibatch reactors for specialty chemicals (Srinivasan and Bonvin, 2006; Bonvin et al., 2006), polymerization reactors (François et al., 2004; Bonvin et al., 2005; Chatzidoukas et al., 2005), bioreactors (Kadam et al., 2006), and batch-distillation columns (Welz et al., 2006a; Welz et al., 2006b).

Industrial Polymerization Process

An industrial polymerization process is considered as a case study example. The problem has been introduced by Bayer AG as a test case during the research project INCOOP (http://www.lpt.rwth-aachen.de/Research/Completed/co_incoop.php; Kadam et al. (2003)). For confidentiality reasons, we sketch the process, leaving out most of the proprietary details. Furthermore, process variables are consistently scaled throughout the article.

Process description

The flow sheet of this large-scale continuous polymerization process is shown in Figure 3. The exothermic polymerization involving multiple reactions takes place in a continu-

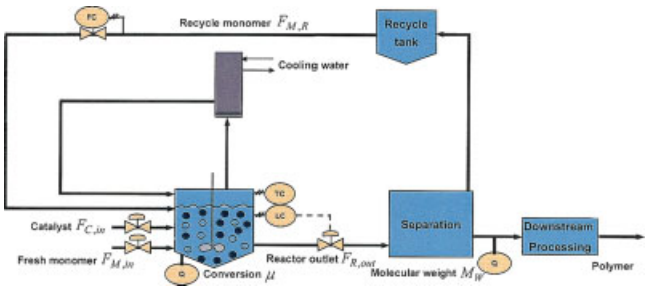

Figure 3. Simplified process flow sheet.

[Color figure can be viewed in the online issue, which is available at www.interscience.wiley.com.]

ously stirred-tank reactor (CSTR) equipped with an evaporative cooling system. The reactor is operated at an open-loop unstable operating point corresponding to a medium level of conversion, which is stabilized by a temperature controller. The reactor is followed by a separation unit for separating the polymer from unreacted monomer and solvent. Unreacted monomer and solvent go back to the reactor via a recycle tank, while the polymer melt is sent to downstream processing and blending units. The end-user properties can be related to polymer viscosity and polymer content in the reactor that are either directly measured or inferred from concentration measurements.

Process model

A rigorous reactor model is available from previous studies at Bayer AG (Dünnebier et al., 2004; Dünnebier et al., 2005). The reactor and recycle tank are modeled in detail, while the separation unit and the condenser are simplified significantly using process insight. This way the major dynamics of the process are captured while keeping the complexity of the model at a reasonable level. The reactor is modeled as a continuous stirred-tank reactor (CSTR), with mass and energy balances and complex polymerization kinetics for all components involved. The separator is modeled as a static splitter. The condenser model is a grey box model, comprising static mass balances combined with a second-order linear dynamic model identified from process data. The reaction kinetics result in open-loop unstable temperature dynamics at the nominal operating point. To prevent any temperature disturbance causing either a quench down to the low-temperature steady-state, corresponding to low-conversion, or runaway up to the high-temperature steady-state corresponding to high-conversion, a feedback control scheme for the reactor temperature is required. Therefore, a stabilizing PID-type controller for the reactor temperature is implemented in the model. The reactor holdup is maintained using a proportional controller that manipulates the reactor outlet flowrate. The model is implemented in the dynamic simulation software gPROMS (gPROMS, 2002). The dynamic process model consists of 200 differential and 2,500 algebraic equations. The model cannot be stated in this article for both space and confidentiality reasons.

Measurements

As in most quality control problems, the availability of reliable measurements is crucial for successful implementation. For a certain class of polymerization problems, the end-user quality variables can be inferred from other measurements (for example viscosity, concentrations) using a model. Therefore, quality control often relies on some type of soft sensor. For this process, the following measurements or model-based estimates are considered to be available in this study:

- flow rates of recycle and fresh monomers, $F_{M,R}$ and $F_{M,in}$,
- flow rate of reactor outlet $F_{R,out}$,
- reactor temperature T_R, and holdup V_R,
- recycle tank holdup V_{RT},
- reactor solvent concentration C_s,
- reactor conversion μ,
- polymer molecular weight M_W.

Grade Transition via Numerical Optimization

Problem formulation

The task is to perform a change from polymer grade A of molecular weight $\overline{M}_{W,A} = 0.727$, and reactor conversion $\bar{\mu}_A = 1.0$ to grade B of molecular weight $\overline{M}_{W,B} = 1.0$, and reactor conversion $\bar{\mu}_B = 1.0$ in minimum time. During the transition, operational constraints are enforced on the state and input variables as shown in Table 2. Additionally, there are endpoint constraints on the reactor conversion μ, and the polymer molecular weight M_W that are more strict than those enforced during the transition.

Three input variables $\boldsymbol{u}$ are available: The flowrate of fresh monomer $F_{M,in}$, the flowrate of recycled monomer $F_{M,R}$, and the catalyst feed stream $F_{C,in}$. In addition, the transition time t_f, which represents the objective function to be minimized, is also a (scalar) decision variable. Note that the reactor holdup is maintained at constant setpoint by adjusting the reactor outlet flow rate. The dynamic optimization problem is formulated mathematically as

$$\min_{F_{M,in}(t), F_{M,R}(t), F_{C,in}(t), t_f} t_f, \qquad (\mathrm{P_e})$$

$$\text{s. t.} \quad \text{DAE process model} \qquad (11)$$

$$F^L_{R,out} \le F_{R,out}(t) \le F^U_{R,out} \qquad (12)$$

$$V^L_{RT} \le V_{RT}(t) \le V^U_{RT} \qquad (13)$$

$$\mu^L \le \mu(t) \le \mu^U \qquad (14)$$

$$M^L_W \le M_W(t) \le M^U_W \qquad (15)$$

Table 2. Constrained Variables and Scaled Values of the Corresponding Bounds

Lower Bounds	Constrained Variables	Upper Bounds
0	Reactor outlet flowrate $F_{R,out}$	1
0	Recycle tank holdup V_{RT}	1
0.875	Reactor conversion μ	1.031
0.713	Polymer molecular weight M_W	1.054
1	Reactor solvent concentration C_s	2
0.92	Reactor temperature T_R	1.2
0.1	Fresh monomer flowrate $F_{M,in}$	1
0	Recycled monomer flowrate $F_{M,R}$	1
0	Fresh catalyst flowrate $F_{C,in}$	1

$$C_s^L \le C_s(t) \le C_s^U \tag{16}$$

$$T_R^L \le T_R(t) \le T_R^U \tag{17}$$

$$F_{M,in}^L \le F_{M,in}(t) \le F_{M,in}^U \tag{18}$$

$$F_{M,R}^L \le F_{M,R}(t) \le F_{M,R}^U \tag{19}$$

$$F_{C,in}^L \le F_{C,in}(t) \le F_{C,in}^U \tag{20}$$

$$M_W(t_f) \ge \overline{M}_{W,B} \tag{21}$$

$$\mu(t_f) \ge \overline{\mu}_B \tag{22}$$

The superscripts L and U denote lower and upper bounds, respectively. In the problem formulation, the transition time t_f is a decision variable. The model has been described in more detail in the Process model section. Once the target polymer grade B has been reached, the process is stabilized at a steady state producing on-specification polymer for a given production rate. This objective of production rate control is not considered in this article, but is discussed elsewhere (Dünnebier et al., 2004).

Characterization of the nominal optimal solution

The optimal grade change problem P_e is solved numerically using the dynamic optimizer DyOS (DyOS, 2002) that uses an adaptive shooting method which is detailed elsewhere (Schlegel et al., 2005; Schlegel and Marquardt, 2006a; Schlegel and Marquardt, 2006b). To find an accurate optimal solution with an identifiable control structure, a wavelet-based adaptive refinement method combined with an automatic control-structure-detection algorithm is applied. Each input profile is parameterized as a piecewise-constant or piecewise-linear function on an adaptively refined discretization grid. A detailed discussion of the computational statistics for this problem can be found elsewhere (Schlegel and Marquardt, 2006a; Schlegel and Marquardt, 2006b).

The optimal input profiles,[1] the corresponding profiles of the polymer quality variables and the state constraints are shown in Figures 4–6. All three input variables reach their bounds for a certain time period during the transition (Figure 4). In addition, the constraints on the reactor outlet flow rate, and the recycle tank holdup are active for some time intervals (Figure 6).

The dynamic optimizer not only calculates the optimal solution, but also automatically detects the input structure by characterizing the optimal input profiles and the active state and endpoint constraints. For technical details on the algorithm, the reader is referred to Schlegel and Marquardt (2006b). The structure of each input is given in Table 3. The arcs are separated by dotted lines in Figures 4–6, and labelled by the tags used in Table 3. The interpretation of the solution for each arc is as follows:

1. Arc 1: The flow rates of fresh monomer $F_{M,in}$, and fresh catalyst $F_{C,in}$, are at their upper and lower bound, respectively, while the flow rate of recycled monomer $F_{M,R}$ is adjusted to keep the upper bound on the reactor outlet flow rate $F_{R,out}$ active (state constraint) (see Figures 4 and 6). It can be observed that $F_{M,R}$ moves towards its lower bound, reaching of which defines the end of Arc 1 at $t = \tau_1$.

2. Arc 2: Since $F_{M,R}$ is constrained at its lower bound, $F_{M,in}$ is now adjusted to keep $F_{R,out}$ at its upper-bound. Furthermore, $F_{C,in}$ is still at its lower-bound. As the recycled monomer is temporarily stored in the recycle tank, its holdup V_{RT} continuously increases and hits the upper-bound, reaching of which defines the end of Arc 2 at $t = \tau_2$ (Figure 6).

3. Arc 3: On Arc 3, $F_{M,R}$ is adjusted to keep V_{RT} at its upper bound. This results in an increase in the total monomer flow rate to the reactor. To maintain the reactor holdup, $F_{M,in}$ is simultaneously reduced to keep $F_{R,out}$ at its upper-bound. At about the same time, $F_{C,in}$ moves away from its lower bound, not to meet an active constraint, but to mini-

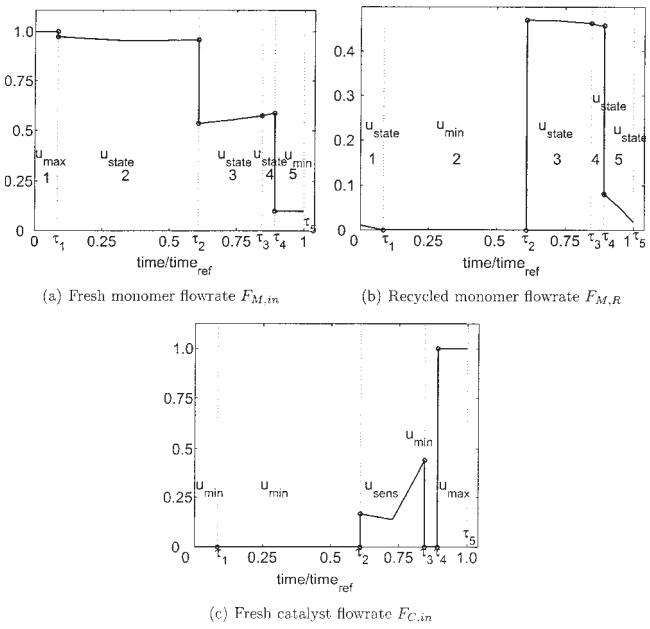

(a) Fresh monomer flowrate $F_{M,in}$ (b) Recycled monomer flowrate $F_{M,R}$

(c) Fresh catalyst flowrate $F_{C,in}$

Figure 4. Optimal profiles of the input variables.

There are 5 arcs in which each input variable can be of the type $\{u_{min}, u_{max}, u_{state}, u_{sens}\}$ depending on whether the corresponding input is at its lower- or upper-bound, determined by a state constraint, or adjusted to implement a compromise that minimizes the objective function (sensitivity-seeking arc).

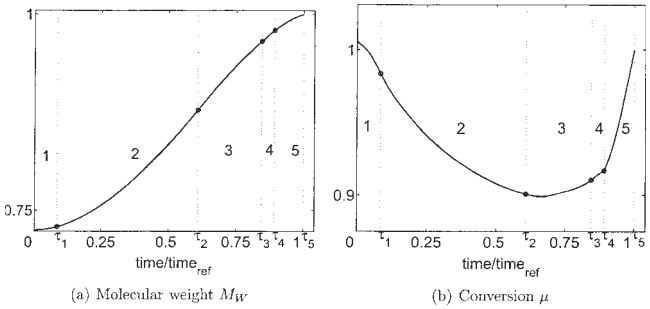

(a) Molecular weight M_W (b) Conversion μ

Figure 5. Optimal profiles of the polymer quality variables.

[1] For confidentiality reasons, both axes in all the solution plots are scaled to 1.

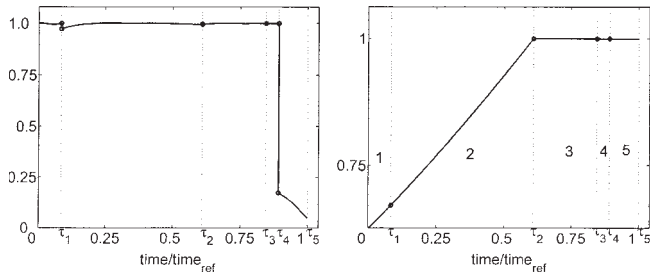

(a) Reactor outlet flowrate $F_{R,out}$ (b) Recycle tank holdup V_{RT}

Figure 6. Optimal profiles of the state constrained variables.

mize the objective function, that is, reduce the transition time. Hence, in this interval, $F_{C,in}$ is a sensitivity-seeking arc.

4. Arc 4: At some time τ_3, the catalyst flow rate $F_{C,in}$ is switched to its lower-bound again. The other inputs $F_{M,in}$ and $F_{M,R}$ continue to seek meeting the state constraints on $F_{R,out}$ and V_{RT}. This drop in $F_{C,in}$ is generated to slow down the increase of molecular weight in preparation for meeting the target value $\overline{M}_{W,B}$ of grade B at the final time t_f.

5. Arc 5: At some later time τ_4, $F_{M,in}$ is switched to its lower bound to increase the reactor-residence time, and, thereby, the conversion μ. As a result, the state constraint on $F_{R,out}$ is no longer active. The constraint on V_{RT} is kept active by continuing to adjust $F_{M,R}$. At about the same time τ_4, $F_{C,in}$ is switched to its upper bound, resulting in a sharp increase in conversion as shown in Figure 5. Both M_W and μ reach their final value $M_{W,B}$ and $\bar{\mu}_B$ at the final time t_f. The switching times τ_3 and τ_4, and the final time t_f are chosen such that the two terminal constraints are met exactly at final time, and the transition time is minimized.

Note that two different types of events happen at both τ_2 and τ_4. At τ_2, $F_{M,R}$ increases sharply to maintain the level of the recycle tank at its upper-bound and $F_{C,in}$ increases to improve the objective function. These two events are not necessarily connected, but they happen to take place at about the same time. Similarly at τ_4, $F_{M,R}$ is reduced sharply to increase the reactor residence time and $F_{C,in}$ goes to its upper bound to increase the conversion. Based on the very similar numerical values that have been computed for the occurrence of the two events around the time τ_2, it was decided to use τ_2 to characterize the simultaneous beginning of both events. The same consideration was done for the two events around the time τ_4.

The characterization of the optimal solution provides a very useful insight into the optimal grade transition. It must be emphasized that this follows from the availability of a process model, and the possibility to compute the corresponding optimal solution and to automatically characterize the types of arcs. In the absence of a nominal optimal solution, educated physical insight and knowledge regarding good practice may allow this type of characterization. However, this is rarely the case in an industrial scenario, especially in the presence of uncertainty. The characterization of the nominal optimal solution will be exploited next to move the process towards optimality in the presence of uncertainty using process measurements.

Optimal Grade Transition via NCO Tracking

Solution model

A solution model can be derived from the characterization of the nominal optimal solution presented in the previous section. The input structure is complex and involves five distinct time intervals. Some of the arcs contribute little to the optimality of the solution, that is, to the reduction of transition time. It is important to realize that approximations can be introduced at this point since the solution model is simply a vehicle to enforce approximate optimality to the true plant. Four such simplifications are introduced next:

1. In Arc 1, $F_{R,out}$ is maintained at its upper bound by adjusting $F_{M,R}$. At the end of this short arc, when $F_{M,R}$ reaches its lower-bound, $F_{M,in}$ is adjusted for the same purpose. To simplify the structure, Arc 1 is omitted, that is, $F_{M,R}$ is fixed at its lower bound right from the beginning of the transition, and $F_{M,in}$ is adjusted to keep $F_{R,out}$ at its upper-bound.

2. The optimal profile of $F_{C,in}$ consists of five successive arcs: minimum, minimum, sensitivity, minimum and maximum. Arc 3 and 5 are there to feed fresh catalyst into the reactor. $F_{C,in}$ is approximated by two piecewise-constant intervals of value $F_{C,in}^0$, starting at time $t = 0$ and $F_{C,in}^{\tau_4}$ starting at $t = \tau_4$.

3. Since, after the transition, the process will be controlled at steady state for grade B, the inputs $F_{M,in}$ and $F_{C,in}$ in Arc 5 are fixed at the values (denoted by the superscript τ_4) corresponding to the desired subsequent target production rate. Note that the inputs $F_{M,in}$ and $F_{C,in}$ correspond to the inlet flow rates that determine the steady-state operating point.

4. For ensuring that M_W moves continuously towards the grade B specifications, it is helpful to enforce an additional constraint on the slope of M_W.

It has been verified via numerical optimization that these approximations bearly increase the transition time, while still

Table 3. Structure of the Optimal Grade Transition

Arc k	Interval $[\tau_{k-1}, \tau_k]$	Input $F_{M,in}(t)$	Input $F_{M,R}(t)$	Input $F_{C,in}(t)$	$F_{R,out}$ (t)	V_{RT} (t)	M_W (t_f)	μ (t_f)
1	[0, 0.09]	max	**state**	min	**active**			
2	[0.09, 0.61]	**state**	min	min	**active**			
3	[0.61, 0.85]	**state**	*state*	sens	**active**	*active*		
4	[0.85, 0.89]	**state**	*state*	min	**active**	*active*		
5	[0.89, 1.0]	min	*state*	max		*active*		
	$t_f = 1.0$						active	active

In a given arc, an input can be on its bound (min or max), determined by a state constraint (state), or such as to minimize the objective function (sens). The relationships between the input variables and the active constraints $F_{R,out}^U$ and V_{RT}^U are indicated in bold and italics, respectively.

Table 4. NCO for the simplified grade transition problem

	Path Objectives	Pointwise Objectives
Constraints	$F_{R,out}[0, \tau_4] = F^U_{R,out}$ $F_{M,R}[0, \tau_2] = F^L_{M,R}$ $V_{RT}[\tau_2, t_f] = V^U_{RT}$	$V_{RT}(\tau_2) = V^U_{RT}$ $M_W(t_f) = \bar{M}_{W,B}$ $\mu(t_f) = \bar{\mu}_B$ $\min[M_W(0, \tau_4)] = s^L$
Sensitivities	-	-

guaranteeing feasible operation. With these approximations, the switching structure reduces to three *intervals*: Interval I_a (Arcs 1 and 2, $0 \le t < \tau_2$), Interval I_b (Arcs 3 and 4, $\tau_2 \le t < \tau_4$), and Interval I_c (Arc 5, $\tau_4 \le t < t_f$), with the corresponding switching times τ_2, τ_4 and t_f. The decision variables (degrees of freedom) are now: $F_{M,in}[0, \tau_4]$, $F_{M,R}[0, \tau_2]$, $F_{M,R}[\tau_2, t_f]$, $F^0_{C,in}$, τ_2, τ_4 and t_f, for which optimality conditions need to be established. Note that $F_{M,in}[\tau_4, t_f]$ and $F_{C,in}[\tau_4, t_f]$ are no longer decision variables since they are fixed at the known values $F^{\tau_4}_{M,in}$ and $F^{\tau_4}_{C,in}$, respectively. The NCO corresponding to the simplified problem are given in Table 4. It is clearly seen that, with the approximations that have been introduced, there are no sensitivity-seeking elements, that is, the optimal solution is entirely determined by active constraints. Note that the pointwise constraints involve elements that are active either during the run or at run end.

Using the steps described in the NCO tracking using a solution section, a solution model is derived by linking the decision variables (the various intervals and switching times of the inputs) to the NCO of the corresponding optimization problem. The resulting solution model reads

$$F_{M,in}(t) = \begin{cases} \mathcal{K}_{F_{R,out}}(F_{R,out}(t), F^U_{R,out}) & \text{for } 0 \le t < \tau_4 \ (I_a, I_b) \\ F^{\tau 4}_{M,in} & \text{for } \tau_4 \le t < t_f \ (I_c) \end{cases} \quad (23)$$

$$F_{M,R}(t) = \begin{cases} F^L_{M,R} & \text{for } 0 \le t < \tau_2 \quad (I_a) \\ \mathcal{K}_{v_{RT}}(V_{RT}(t), V^U_{RT}) & \text{for } \tau_2 \le t < t_f \ (I_b, I_c) \end{cases} \quad (24)$$

$$F_{C,in}(t) = \begin{cases} F^0_{C,in} & \text{for } 0 \le t < \tau_4 \ (I_a, I_b) \\ F^{\tau_4}_{C,in} & \text{for } \tau_4 \le t < t_f \ (I_c) \end{cases} \quad (25)$$

$$V_{RT}(\tau_2) = V^U_{RT} \quad \text{defines } \tau_2 \quad (26)$$

$$M^{pred}_{W,B}(\tau_4) = _{W,B} \quad \text{defines } \tau_4 \quad (27)$$

$$\mu(t_f) = \bar{\mu}_B \quad \text{defines } t_f \quad (28)$$

$$F^0_{C,in} = \mathcal{R}_{F^0_{C,in}}(\min(\dot{M}_W(t)), s^L) \quad \text{for } 0 \le t < \tau_4 \quad (29)$$

$$M^{pred}_{W,B}(t) = g(M_W(t), \dot{M}_W(t), (\mu(t) - \bar{\mu}_B)). \quad (30)$$

$\mathcal{K}$ and $\mathcal{R}$ are online and run-to-run controllers, respectively, that are used to implement the decentralized control structure given by the solution model. τ_2, τ_4 and t_f are defined by Eqs. 26–28 as the times t that meets the corresponding conditions. The parameter s^L is the minimum slope to be guaranteed for $\dot{M}_W$ in the interval $[0, T_4)$. $M^{pred}_{W,B}(t)$ is the value of $M_W(t_f)$ that is predicted at time t.

The different parts of the adjustable inputs are discussed next:

- *Parts determined by path constraints*

Fixed parts. $F_{M,R}$ is fixed at its lower bound $F^L_{M,R}$ in Interval I_a. In Interval I_c, the inlet flow rates $F_{M,in}$ and $F_{C,in}$ are fixed at values corresponding to the steady-state target production rate, that is, $F^{\tau_4}_{M,in}$and $F^{\tau_4}_{C,in}$, respectively. The steady-state values of the inputs are calculated by performing a steady-state simulation at the target production rate for grade B.

Adjustable parts. Only the constraints on $F_{R,out}$ and V_{RT} are active during some of the intervals. In Intervals I_a and I_b, $F^U_{R,out}$ is kept active by adjusting $F_{M,in}$ using the controller $\mathcal{K}_{F_{R,out}}$ and, in Intervals I_b and I_c, V^U_{RT} is kept active by adjusting $F_{M,R}$ using the controller $\mathcal{K}_{V_{RT}}$. Depending on the nature of the control problem, PID-type or model-based controllers can be implemented (see implementation details in the Appendix).

- *Parts determined by pointwise constraints*

During the run. The parameter τ_2 is determined implicitly upon reaching the constraint V^U_{RT}. Furthermore, in Intervals I_a and I_b, $F_{C,in}(t) = F^0_{C,in}$. The value $F^0_{C,in}$ is adapted on a run-to-run basis such that the minimum slope of $M_W(t)$ reaches the constraint s^L. The value $s^L = 0.1$ was determined by trial and error so as to easily reach the target $\bar{M}_{W,B}$ at the end of the transition (see implementation details in the Appendix).

At run end. According to the optimality conditions, both endpoint constraints $M_W(t_f) = \bar{M}_{W,B}$ and $\mu(t_f) = \bar{\mu}_B$ are active at t_f. For implementation purposes, the switching time τ_4 is linked to $\bar{M}_{W,B}$ and t_f to $\bar{M}_B$. The determination of τ_4 requires a prediction, at time t, of the value of $M_W(t_f)$ as given by the formal model (Eq. 30). Then, τ_4 is the first value of t for which $M^{pred}_{W,B}(t) = \bar{M}_{W,B}$ (see implementation details in the Appendix).

Superstructure solution model

The state constraints on reactor conversion $\mu(t)$, solvent concentration $C_s(t)$ and reactor temperature $T_R(t)$ are not active during the transition under nominal conditions. However, in the presence of uncertainty related to the initial conditions, state constraints on both reactor conversion and solvent concentration might become active. Hence, all constrained quantities are monitored for possible activation. This scenario can be addressed by extending the solution model as follows

$$F_{M,in}(t) = \begin{cases} \mathcal{K}_{F_{R,out}}(F_{R,out}(t), F^{des}_{R,out}(t)) & \text{for } 0 \le t < \tau_4 \ (I_a, I_b) \\ F^{\tau_4}_{M,in} & \text{for } \tau_4 \le t < t_f \ (I_c) \end{cases} \quad (31)$$

$$F_{M,R}(t) = \begin{cases} F^L_{M,R} & \text{for } 0 \le t < \tau_2 \quad (I_a) \\ \mathcal{K}_{V_{RT}}(V_{RT}(t), V^U_{RT}) & \text{for } \tau_{V_{RT}} \le t < \tau_{C_s} \quad (I_b, I_c) \\ \mathcal{K}_{C_s}(C_s(t), C^L_s) & \text{for } \tau_{C_s} \le t < \tau_{V_{RT}} \quad (I_b, I_c) \end{cases} \quad (32)$$

$$F_{C,in}(t) = \begin{cases} F^0_{C,in} & \text{for } 0 \le t < t_4 \quad (I_a, I_b) \\ F^{\tau_4}_{C,in} & \text{for } \tau_4 \le t < t_f \quad (I_c) \end{cases} \quad (33)$$

$$\mu(\tau_\mu) = \mu^L \qquad \text{defines } \tau_\mu \tag{34}$$

$$V_{RT}(\tau_{V_{RT}}) = V_{RT}^U \qquad \text{defines } \tau_{V_{RT}} \tag{35}$$

$$C_s(\tau_{C_s}) = C_s^L \qquad \text{defines } \tau_{C_s} \tag{36}$$

$$\tau_2 = \min(\tau_{V_{RT};}\, \tau_{C_s}) \qquad \text{defines } \tau_2 \tag{37}$$

$$M_{W,B}^{pred}(\tau_4) = \overline{M}_{W,B} \qquad \text{defines } \tau_4 \tag{38}$$

$$\mu(t_f) = \overline{\mu}_B \qquad \text{defines } t_f \tag{39}$$

$$F_{R,out}^{des}(t) = \begin{cases} F_{R,out}^U & \text{for} \quad 0 \le t < \tau_\mu \\ \mathcal{K}_\mu(\mu(t), \mu^L) & \text{for} \quad \tau_\mu \le t < \tau_4 \end{cases} \tag{40}$$

$$F_{C,in}^0 = \mathcal{R}_{F_{C,in}^0}(\min(\dot{M}_W(t)), s^L) \quad \text{for} \quad 0 \le t < \tau_4 \tag{41}$$

$$M_{W,B}^{pred}(t) = g(M_W(t), \dot{M}_W(t), (\mu(t) - \overline{\mu}_B)). \tag{42}$$

This superstructure solution model adds the following elements to the solution model Eqs. 23–30 derived from the nominal optimal solution:

• *Constraints on* μ. In Intervals I_a and I_b, the input $F_{M,in}$ is adjusted to meet the desired value $F_{R,out}^{des}$ that does not allow the reactor conversion μ to drop below the lower limit μ^L (cf. Eq. 40). $\mathcal{K}_\mu$ is an on-line controller that adjusts $F_{R,out}^{des}$ to keep μ at its lower-bound μ^L. The activation time of the constraint on μ is denoted by τ_μ (cf. Eq. 34). Note that if $\tau_\mu \ge \tau_4$, the constraint on μ does not become active.

• *Constraints on* C_s. In Intervals I_b and I_c, $F_{M,R}$ is linked to the constraint on solvent concentration C_s^L in addition to that on recycle tank holdup V_{RT}^U (cf. Eq. 32). Only one of the constraints (and corresponding controllers) is active at the same time, that is, the more restrictive of the two. The switching time τ_2 is determined implicitly upon reaching the constraint on either V_{RT} or C_s (cf. Eq. 37). The activation times of the constraints on V_{RT} and C_s are denoted by $\tau_{V_{RT}}$ and τ_{C_s}, respectively (cf. Eqs. 35 and 36). Note that if $\tau_2 \ge \tau_4$, the constraints on V_{RT} and C_s do not become active.

Reliable on-line measurements or estimates of the constrained variables ($F_{R,out}$, V_{RT}, M_W, $\dot{M}_W$, μ, C_s) are necessary for implementing the NCO-tracking strategy using the superstructure solution model. Obviously, the required estimators add to the complexity of the NCO-tracking solution. However, estimation of unmeasured process quantities is also necessary for almost any alternative model-based control approach. The input-output links in the solution model are implemented using the feedback controllers $\mathcal{K}$ and $\mathcal{R}$, in this study PI-type controllers, with the nominal optimal input profiles used as feedforward signals. Advanced controllers could also be used for improved tracking performance (Dünnebier et al., 2004).

In the designed control superstructure, depending upon the state of the process, one controller *overrides* the other. In the process control terminology, this type of control structure is referred to as *overriding* or *signal-select* controller (Luyben and Luyben, 1997). The process with the proposed control superstructure is shown in Figure 7. State-event-based triggers are used for implementing the superstructure decisions. The logic behind the triggers is presented as a flowsheet in Figure 8 in which, for the sake of simplicity, the time dependence of the variables is omitted. The logic needs to be simultaneously re-evaluated at each sampling interval Δt.

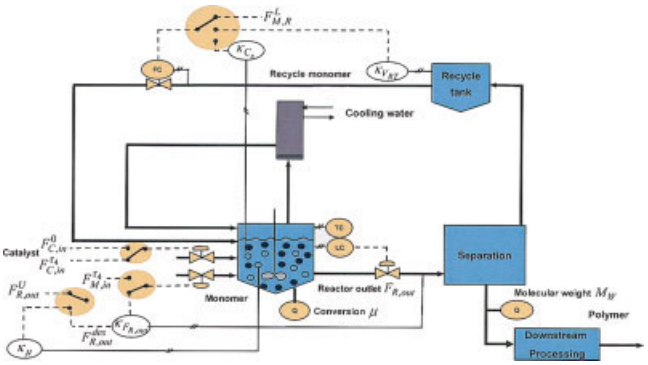

Figure 7. Process with the on-line NCO-tracking controllers and the triggers.

[Color figure can be viewed in the online issue, which is available at www.interscience.wiley.com.]

NCO-tracking results

This polymerization process has inherent operational uncertainty. As part of this investigation, a considerable amount of uncertainty in the form of different initial conditions is considered. On the other hand, measurement noise is not considered. This section compares the optimal solutions obtained via NCO tracking for various cases, and then evaluates the performance of the NCO-tracking scheme.

Nominal and perturbed cases

The NCO-tracking superstructure for optimal grade transition is tested using the simulated plant model for two different cases:

1. *Nominal case*. The input profiles are adjusted using measurements according to the model Eqs. 23–30 or, equivalently, model Eqs. 31–42, since there is no change in the set of active constraints. The NCO-tracking profiles are depicted by solid lines in Figures 9–11. The profiles of the inputs and constrained variables are very similar to those computed numerically using the nominal model (see Figures 4–6). The approximations introduced as part of the NCO-tracking strategy increase the transition time by only 0.8%.

2. *Perturbed case*. The NCO-tracking superstructure is used for grade transition with different initial conditions that result from a different-than-nominal solvent concentration. As much as 20% change in solvent concentration is expected. The input and constrained variable profiles are depicted by dash-dotted lines in Figures 9–11. The optimal profiles for the perturbed case (+20% change in solvent concentration) differ significantly from those for the nominal case. Also, the transition time t_f is considerably larger. The nominally inactive path constraint on μ becomes active (Figure 10b) in this case. When this constraint becomes active, the reactor outlet flowrate is adjusted to keep μ close to its lower bound μ^L as shown in Figure 11a. As a simple PID controller tuned for the nominal case is used, tight control of μ at the constraint is not possible, which results in an

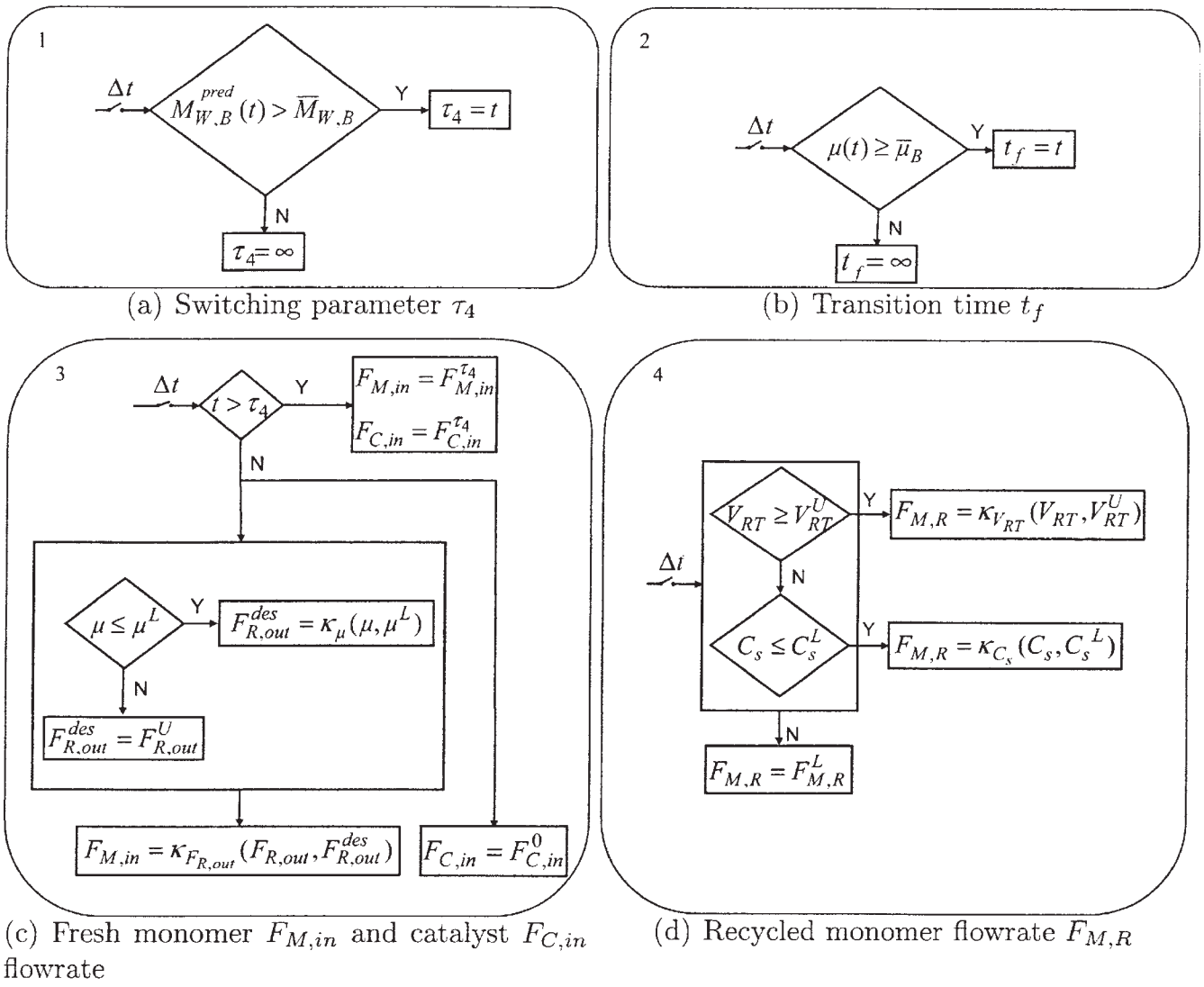

Figure 8. Logic for the solution model and the trigger mechanism.

offset. Furthermore, the slope of the M_W-profile decreases significantly in Interval I_c, while μ increases linearly. This fact, together with measurements of M_W, $\dot{M}_W$ and μ or estimates, thereof, are used by the empirical model (Eq. 42) to predict $M_W(t_f)$. Adaptation of τ_4 is crucial for meeting the terminal constraints on M_W and μ.

Also, note that open-loop application of the nominal solution to the perturbed case is infeasible, which illustrates the need to use online optimization.

Performance of NCO-tracking scheme

In Table 5, the performance of the NCO-tracking scheme is compared to a robust solution, and to numerical optimization assuming perfect knowledge of the perturbation. The robust solution, which corresponds to common industrial practice, represents a single strategy that is computed off-line and needs to be feasible for both the nominal and perturbed cases. Hence, it is clearly less performant than the nominal optimal solution ($t_f \geq 5$). The NCO-tracking approach is computed using the decentralized control structure presented in this work. Finally, the ideal solution corresponds to the best possible solution that is computed numerically using full knowledge of the perturbation. Table 5 shows that, due the large perturbation, the robust solution is rather poor. In contrast, NCO tracking comes very close to the ideal solution, and this without knowledge of the perturbation but at the expense of on-line measurements and (possibly) state estimation.

These simulation results have demonstrated that a decentralized control strategy using a solution model and measurements can implement a complex grade transition nearly optimally. At this stage, it must be re-emphasized that the generation of the solution model, as well as its superstructure requires the optimal solution for the nominal case and additional process insights. Furthermore, stability and integrity of the decentralized control system cannot be guaranteed by the current state of our research. However, the expected economic benefits in terms of transition time reduction, and thus the amount of off-specification material, is quite significant compared to the conventional approach practiced in the plant.

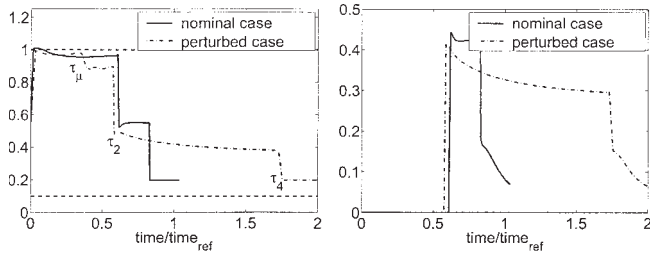

(a) Fresh monomer flowrate $F_{M,in}$ (b) Recycled monomer flowrate $F_{M,R}$

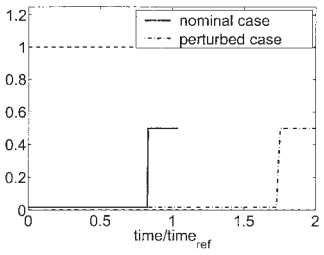

(c) Fresh catalyst flowrate $F_{C,in}$

Figure 9. Optimal profiles of the input variables obtained using NCO tracking.

The perturbation corresponds to a change in solvent concentration, and slows down the grade transition considerably.

For limited grade transition scenarios, nominal optimal solutions can be calculated offline and NCO tracking implemented online. Hence, the problem of process model maintenance is simplified to a certain extent.

Conclusion

This article has addressed the applicability of the NCO-tracking approach proposed by Srinivasan et al. (2003a) to a complex simulated industrial polymerization process. The NCO are tracked using a decentralized overriding control structure expressed in the form of a solution model. As long as the uncertainty (model mismatch and perturbations) does not change the structure of the optimal solution, that is, the type and sequence of arcs, NCO-tracking allows implementing feasible and near-optimal operation, even in the presence of uncertainty. The solution model consists of state-event-triggered controllers sequenced according to the structure of the optimal solution.

The optimal profiles of three input variables exhibit a complex structure involving several active path and terminal constraints. The off-line computed optimal solution shows significant reduction in transition time and off-specification polymer production when compared to the conventional strategies used by operators. However, off-line implementation of the nominal optimal solution is inappropriate in the presence of the uncertainty that is typically experienced in polymerization processes. In this study, the uncertainty is associated with the unknown initial state of the process due to different solvent concentration. A solution model is generated from the nominal optimal solution, and a control superstructure is considered to handle the possible activation of nominally-inactive path constraints. Simple PI-type controllers are used to implement the solution model. For two different perturbation scenarios, simulation of the NCO-tracking approach shows that considerable reduction in transition time is possible, while still guaranteeing feasible operation. The control strategy that enforces (near) optimality under uncertainty is simple to implement in real-time.

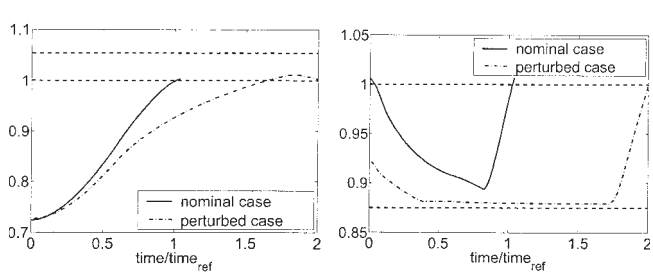

(a) Polymer molecular weight M_W (b) Reactor conversion μ

Figure 10. Profiles of the polymer quality variables obtained using NCO tracking.

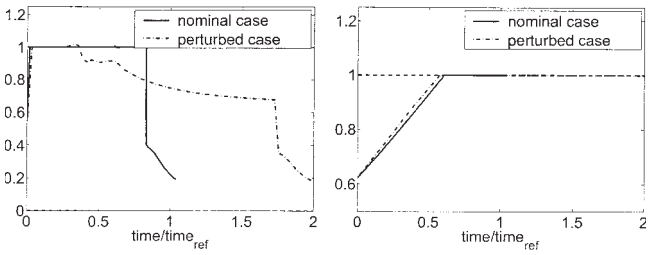

(a) Reactor outlet flowrate $F_{R,out}$ (b) Recycle tank holdup V_{HT}

Figure 11. Profiles of the state constrained variables obtained using NCO tracking.

However, this does not come for free. Though a process model is not used for on-line implementation, reliable measurements of quality and constrained variables are necessary. If measurements are not directly available, state estimation may be necessary. Moreover, it was assumed that the solution (super)structure remains valid for different types of uncertainty. When this assumption cannot be made, the problem is considerably more difficult to solve via NCO tracking. Finally, in order to be able to handle various operational problems, the NCO-tracking approach could be best integrated in a more general framework for dynamic optimization and control that uses both a process model and a solution model. This is clearly an interesting direction for future research.

Table 5. Transition Times Using Different Optimization Strategies

Case	Robust Solution (Perturbation Unknown)	NCO Tracking (Perturbation Unknown)	Ideal Solution (Perturbation Known)
Nominal	≥5	1.008	1.0
Perturbation 1 (+20% solvent concentration)	≥5	2.03	1.81
Perturbation 2 (−20% solvent concentration)	≥5	0.938	0.915

Two distinct perturbations are considered, each with different initial solvent concentration.

Acknowledgment

The authors would like to thank Dr. Karsten-U. Klatt and Dr. Guido Dünnebier of Bayer Technology Services, Germany for making available a process model and their support of this work.

Literature Cited

Biegler, L. T., A. M. Cervantes, and A. Wächter. "Advances in Simultaneous Strategies for Dynamic Process Optimization." *Chem. Eng. Sci.* **24**, 39–51 (2002).

Binder, T., L. Blank, H. G. Bock, R. Burlisch, W. Dahmen, M. Diehl, T. Kronseder, W. Marquardt, and J. P. Schlöder. *Online Optimization of Large Scale Systems*. Chap. Introduction to Model-based Optimization of Chemical Processes on Moving Horizons, Springer pp. 295–339 (2001).

Bock, H. G., M. M. Diehl, D. B. Leineweber, and J. P. Schlöder. A direct multiple shooting method for real-time optimization of nonlinear DAE processes. In: *Non-linear Model Predictive Control* F. Allgöwer and A. Zheng, eds. Birkhäuser Verlag. Basel, pp. 246–267 (2000).

Böhm, L. L., P. Göbel, O. Lorenz, and T. Tauchnitz. Pe-hd Production Control using a Complex Model Based State Observer. *DECHEMA Monographs*, **127**, 257–273 (1992).

Bonvin, D., B. Srinivasan, and D. Hunkeler. Control and Optimization of Batch processes: Improvement of Process Operation in the Production of Specialty Chemicals. *IEEE Control Systems Magazine*. In press (2006).

Bonvin, D., L. Bodizs, and B. Srinivasan. Optimal grade transition for polyethylene reactors via NCO. *Trans IChemE Part A: Chem. Eng. Res. and Design*. **83(A6)**, 692–697 (2005).

Bryson, A. E., and Y.-C. Ho. Applied Optimal Control. Taylor & Francis. Bristol, PA. (1975).

Chatzidoukas, C., C. Kiparissides, B. Srinivasan, and D. Bonvin. Optimization of Grade Transitions in an Industrial Gas-Phase Polymerization Reactor via NCO Tracking. In: Proc. of IFAC World Congress. Prague (2005).

Congalidis, J. P., and J. R. Richards. "Process Control of Polymerization Reactors: an Industrial Perspective." *Polymer Reaction Eng.* **6**, 71–111 (1998).

Diehl, M., H. G. Bock, J. P. Schloder, R. Findeisen, Z. Nagy, and F. Allgower. "Real-Time Optimization and Nonlinear Model Predictive Control of Processes Governed by Differential-Algebraic Equations." *J. of Process Control*. **12(4)**, 577–585 (2002).

Dittmar, R., and G. D. Martin. "Nichtlineare modellgestützte prädiktive Regelung eines industriellen Polypropylenreaktors unter Verwendung Künstlicher neuronaler Netze." *atp*. **43**, 2–11 (1997).

Dünnebier, G., D. van Hessem, J. V. Kadam, K.-U. Klatt, and M. Schlegel. "Prozessführung und Optimierung von Polymerisationsprozessen." *Chemie Ingenieur Technik*. **76(6)**, 703–708 (2004).

Dünnebier, G., D. van Hessem, J. V. Kadam, K.-U. Klatt, and M. Schlegel. Optimization and control of polymerization processes. *Chem Eng & Technol*. **28(5)**, pp. 575 (2005).

DyOS. DyOS User Manual, Release 2.1. Lehrstuhl für Prozesstechnik, RWTH Aachen University. Aachen (2002).

Embirucu, M., E. L. Lima, and J. C. Pinto. "A Survey of Advanced Control of Polymerization Reactors." *Polymer Eng. and Sci.* **36**, 433–447 (1996).

François, G., B. Srinivasan, D. Bonvin, J. B. Hernandas, and D. Hunkler. "Run-to-Run Adaptation of a Semiadiabatic Policy for the Optimization of an Industrial Batch Polymerization process." *Ind. Eng. Chem. Res*. **43(23)**, 7238–7242 (2004).

gPROMS. gPROMS User Guide (Release 2.1.1). Process Systems Enterprise Ltd., London, U.K. (2002).

Kadam, J. V., W. Marquardt, M. Schlegel, O. H. Bosgra T. Backx, P.-J. Brouwer, G. Dünnebier, D. van Hessem, A. Tiagounov, and S. de Wolf. Towards integrated dynamic real-time optimization and control of industrial processes. In: Proc. of FOCAPO 2003. I. E. Grossmann and C. M. McDonald, eds. pp. 593–596 (2003).

Kadam, J. V., W. Marquardt, M. Schlegel, R. L. Tousain, D. H. van Hessem, J. van den Berg, and O. H. Bosgra. A two-level strategy of integrated optimization and control of industrial processes: a case study. In: European Symposium on Computer Aided Process Engineering – 12. J. Grievink and J. v. Schijndel, eds. Elsevier. pp. 511–516 (2002).

Kadam, J. V., M. Schlegel, B. Srinivasan, D. Bonvin, and W. Marquardt. "Dynamic Optimization in the Presence of Uncertainty: From Off-line Nominal Solution to Measurement-Based Implementation." *J. Proc. Contr*. In press (2006).

Kiparissides, C., G. Verros, and J. F. McGregor. "Mathematical Modeling, Optimization, and Quality Control of High-Pressure Ethylene Polymerization Reactors." *Macromol. Chem. Phys.* **33**, 437–527 (1997).

Luyben, M. L., and W. L. Luyben. Essentials of Process Control. McGraw-Hill. New York, USA (1997).

McAuley, K. B., and J. F. MacGregor. "On-Line Inference of Polymer Properties in an Industrial Polyethylene Reactor." *AIChE J*. **37**, 825–835 (1991).

McAuley, K. B., and J. F. MacGregor. "Optimal Grade Transitions in a Gas-Phase Polyethylene Reactor." *AIChE J*. **38**, 1564–1576 (1992).

Mutha, R. K., W. R. Cluett, and A. Penlidis. "On-line nonlinear model-based estimation and control of a polymer reactor. *AIChE J*. **43**, 3042–3058 (1997).

Na, S. S., and H.-K. Rhee. An Exprimental Study for Property Control in a Continous Styrene Polymerization Reactor Using a Polynomial ARMA Model. *Chem. Eng. Sci*. **57**, 1165–1173 (2002).

Ogunnaike, B. A. "On-Line Modelling and Predictive Control of an Industrial Terpolymerization Reactor." *Int. J. Control*. **59**, 711–729 (1994).

Prasad, V., M. Schley, L. P. Russo, and B. W. Bequette. "Product Property and Production Rate Control of Styrene Polymerization." *J. of Process Control* **12**, 353–372 (2002).

Schlegel, M. and W. Marquardt. "Adaptive Switching Structure Detection for the Solution of Dynamic Optimization Problems." *Ind. Eng. Chem. Res*., In press. (2006a).

Schlegel, M. and W. Marquardt. "Detection and Exploitation of the Control Switching Structure in the Solution of Dynamic Optimization Problems." *J. of Process Control*. **16(3)**, 275–290 (2006b).

Schlegel, M., K. Stockmann, T. Binder, and W. Marquardt. "Dynamic Optimization Using Adaptive Control Vector Parameterization." *Comp. Chem. Eng*. **29(8)**, 1731–1751 (2005).

Seki, H., M. Ogawa, S. Ooyama, K. Akamatsu, M. Oshima, and W. Yang. Industrial application of a nonlinear model predictive control to polymerization reactors. *Control Eng. Practice*. **9**, 819–828 (1994).

Srinivasan, B. and D. Bonvin. Dynamic optimization under uncertainty via NCO tracking: A solution model approach. In: Proc. BatchPro Symposium 2004. C. Kiparissides, ed. pp. 17–35 (2004).

Srinivasan, B. and D. Bonvin. "Real-Time Optimization of Batch Processes via Tracking of Necessary Conditions of Optimality." *Ind. Eng. Chem. Res*. In press (2006).

Srinivasan, B., D. Bonvin, E. Visser, and S. Palanki. "Dynamic Optimization of Batch Processes II. Role of Measurements in Handling Uncertainty." *Comput and Chem. Eng*. **27**, 27–44 (2003a).

Srinivasan, B., S. Palanki and D. Bonvin. "Dynamic Optimization of Batch Processes I. Characterization of the Nominal Solution." *Comp. Chem. Eng*. **27**, 1–26 (2003b).

Welz, C., A. G. Marchetti, B. Srinivasan, N. L. Ricker and D. Bonvin. "Validation of a Solution Model for the Optimization of a Batch Distillation Column. *AIChE J*. In press (2006a).

Welz, C., B. Srinivasan, and D. Bonvin. "Measurement-Based Optimization of Batch Processes: Meeting Terminal constraints via Trajectory Following." *J. Proc. Contr*. In press (2006b).

Young, R. E., R. D. Bartusiak, and R. W. Fontaine. "Evolution of an Industrial Nonlinear Model Predictive Controller." *Proc. of Chem Process Control VI* **6**, 119–127 (2002).

Appendix — Implementation aspects

On-line controllers

Continuous-time PID-type controllers with the nominal control (u_{opt}) as feedforward part are used to implement on-line control

$$\mathcal{K}: u(t) = u^{opt}(t) + K(y(t) - y^{sp}) + K_I \int_0^t (y(t) - y^{sp})dt + K_D\dot{y}(t). \tag{A1}$$

Here, $y(t)$ is a measurement quantity with y^{sp} as its setpoint. K, K_I and K_D as its tuning parameters. Constraints on the controls are used as part of the PID algorithm.

Run-to-run controller

An integral controller is used to implement the run-to-run control

$$\mathcal{R} : u_{k+1} = u_k + K(y_k - y^{sp}), \quad \text{for } K = 1, \ldots, n \tag{A2}$$

$$u_0 = u^{opt} \tag{A3}$$

Here, y_k is the measurement quality for run k, and K is the tuning parameter.

Slope of molecular weight

The slope $M_W(t)$ is calculated by computing the filtered value $M_W^f(t)$ using a first-order exponential filter

$$\frac{d}{dt}M_W^f(t) = (M_W(t) - M_W^f(t))/\tau_f, \tag{A4}$$

where τ_f is the filter time constant, and approximating the time derivative $\dot{M}_w(t)$ by $\frac{d}{dt}M_W^f(t)$ given in Eq. A4.

Prediction of final value of molecular weight

The prediction, at time t, of the final value of the molecular weight assumes that the two inlet flow rates $F_{M,in}(t)$ and $F_{C,in}(t)$ are set right away to their final values $F_{M,in}^{\tau_4}$ and $F_{C,in}^{\tau_4}$. The prediction reads

$$M_{W,B}^{pred}(t) = M_W(t) + p\dot{M}_W(t)(\mu(t) - \bar{\mu}_B) \tag{A5}$$

The empirical model uses measurements of $M_W(t)$, its slope $\dot{M}_W(t)$, and the term $(\mu(t) - \bar{\mu}_B)$. The use of the latter term is justified by the finding that, once the two inlet flowrates are set at their final values in Interval I_c, the ratio between the changes in M_W and μ is nearly constant, even in the presence of uncertainty. Note that the parameter p of the empirical model (A5) could be adapted on a run-to-run basis using measurements from past transitions.

Manuscript received Jun. 20, 2006, and revision received Oct. 31, 2006.